Numerical and experimental optimisation of a gravity driven free-surface flow

FRANCISCO[1], M.; LOPES[1] A.M.G. and COSTA[2], V.A.F.
[1]Departamento de Engenharia Mecânica da Faculdade de Ciências e Tecnologia
Universidade de Coimbra
Pinhal de Marrocos, 3030-021 Coimbra
PORTUGAL
[2]Departamento de Engenharia Mecânica
Universidade de Aveiro
Campus Universitário de Santiago, 3819-193 Aveiro
PORTUGAL
[1]miguel.francisco@dem.uc.pt; antonio.gameiro@dem.uc.pt; www.dem.uc.pt
[2]v_costa@mec.ua.pt; www.mec.ua.pt

Abstract: - Water consumption is a major concern nowadays. Water usage in toilets is controlled by more and more demanding specifications. It is important to note that, in average, a 4 person's family makes 20000 water toilet flushes per year, which represents approximately 120000 litres of water. The present work aims at the optimisation of the geometrical characteristics of a discharge valve for WC toilets in order to get a discharge flow rate as high as possible, within the restrictions dictated by production impositions. The study was conducted both numerically and experimentally. The numerical computations were made with ANSYS-CFX-5. A mainly structured mesh with hexahedral elements and a standard compressive model for the transient and advective terms of the volume fraction equation were used to minimize the effects of numerical diffusion. The study was carried out, in a first approach, using a stationary computation. In a second phase, the full transient phenomenon was simulated. Comparison of the computed discharge history with the experimental measurements showed an excellent agreement.

Key-Words: - free-surface flow; 3-D unsteady CFD simulation; water saving.

1 Introduction

Saving water is one effective way of improving ecological product efficiency. Manufacturers are getting aware of this recent global consciousness and need to follow stricter norms to reduce water usage. The objective of this work is to get a trusted methodology combining CFD and experimental data for designing toilet flushing valves, by improving their performance, i.e., reducing pressure drop and augmenting its instantaneous volume flow rate. This study closely followed the European Draft Standard DOC CEN/TC 163/WG3/GAH3 N121 for WC flushing cisterns. According to that Standard, the flushing device should discharge a volume of 6 l of water in a full flush. The volume flow rate was to be measured based on the time difference between two pressure levels acquired during the discharge phenomena, corresponding to 5 and 2 litres of the cistern capacity. As the water free surface level drops during the discharge, velocity increases, presenting a maximum value between these two levels. Important velocity gradients are found near the valve's exit walls were the flow can separate and generate turbulence.

There is, nowadays, a high CFD development for free-surface flows due to its growing importance in many application fields, such as nuclear reactor safety, naval industry, engine design and even food processing [1]-[6]. The challenge is on the search for the best suited combination of meshing types, and transient and advection schemes for the volume of fluid (VOF) scalar equation. The numerical results obtained need to be validated using some experimental data. The present work used a commercial CFD package, ANSYS CFX5, which has a strong background on advanced multiphase flow models, and followed some advices from ECORA's CFD Best Practice Guidelines for CFD code validation [7].

The experimental data used to validate numerical results were volume flow and qualitative flow visualisation.

Non-stationary calculations actually simulate the full discharge process, giving time dependent velocity and pressure fields, free-surface movement and the

volume flow. This approach showed to need a quite large computation time.

As an alternative, valve optimisation was performed based on the pressure drop evaluated in stationary low time cost simulations, using a prescribed constant flow velocity taken from the experimental data. Non-stationary calculations were, then, performed only for the most interesting designs. There is a lack of similar work and experimental data as well, as known by the authors. A common research on flow separation in valve gaps was found in combustion engine inlet valves [6] where quantitative techniques like laser-Doppler anemometry and hot-wire anemometry are mentioned as suited for obtaining detailed quantitative velocity measurements. Those could be the tools to use in a future research to detailed validation of CFD results for the present work.

2   Problem Formulation

2.1   Numerical Challenge
The flushing phenomenon to be simulated is a free-surface, unsteady, 3-D, gravity driven flow.

The CFX-5 code uses fully implicit discretized transport equations in a finite control volume mesh with a coupled velocity-pressure solver. These equations are numerical approaches to the mass, energy and momentum conservation equations.

The challenge was to get the best model approach to the physical water discharge, within the tool's capabilities. Parameters such as boundary conditions, meshing types, modelling schemes and convergence criteria were to be tested in order to choose the best option.

The mesh arrangement is known to play an important role on numerical diffusion. This is particularly important in the present case, where large gradients of the scalar volume of fluid are to be captured for an accurate location of the free surface. Hexahedral elements with perpendicular faces to the fluid motion are less diffusive than unstructured tetrahedral elements but less sensitive to round trajectories.

The CFX-5 package includes several schemes for multiphase flow modelling. For this kind of flow, a homogeneous multiphase model can be used because there is a clear separation between water and air, and no splashing of water nor air bubbles' entrainment occur inside the cistern. There is actually a compressive scheme for the VOF advective terms (introduced by Zwart, Scheuerer, and Bogner [2]) that will be used for its proven ability to reduce numerical diffusion as it is better than Upwind and High Resolution advection schemes. This scheme will be tested with unsteady flow, 3-D geometry, and the use of different meshing types with General Grid Interfaces (GGI).

3   Problem Solution

3.1   Experimental facilities
A water cistern was built with glass walls and acrylic base, for a full perception of the process. Dimensions of the cistern are shown in Table 1. A 5 mm bore pressure intake was made at the bottom of the cistern. This pressure intake was connected to a digital differential pressure transducer SETRA® with a range from -2500 to +2500 Pa and an output from 0 to 5 VDC. This transducer was connected itself to a PC's LPT1 port through a PICO ADC 100 converter and results were read on PICO Log Recorder software. Fig. 1 shows the described facility.

Table 1. Geometric dimensions of water cistern.

Cistern length	400 mm
Cistern width	125 mm
Cistern height	150 mm
6.0 litres height	132 mm
5.0 litres height	112 mm
2.0 litres height	50 mm
Residual height	11 mm
Bottom exit bore	52.3 mm

This software acquired data in a Fast Block mode, at the rate of 100 samples per second, which is largely above the 40Hz lower frequency limit specified in the European standard mentioned above.
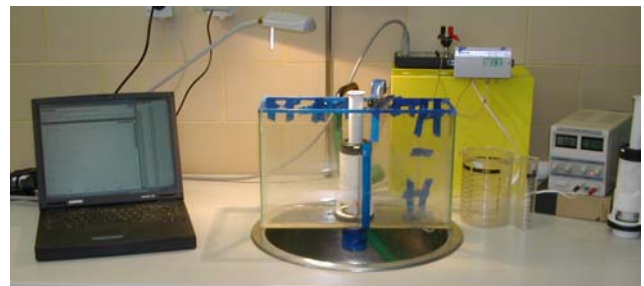

Fig. 1. Experimental installation used to measure volume flow in a 6 litres flushing device.

A mean value of 848,1ms for the time difference between 5 and 2 litres was evaluated after 30 discharges with a standard deviation of 8,29.

The numerical data will next be validated by means of a relative numerical error given by:

$$\varepsilon_{num} = \frac{\Delta t_{exp} - \Delta t_{num}}{\Delta t_{exp}} \times 100 \ [\%] \qquad (1)$$

where Δt_{exp} and Δt_{num} are the experimental and numerical differences between instants t_2 and t_5, respectively.

3.2 Model Selection and Application

Mesh studies were performed considering a simple geometry, which consisted on a simple ¼ rectangular cistern with a circular exit centred at the bottom The results obtained for a flush on a simple unstructured mesh with maximum edge lengths of 10, 5 and 2.5 mm are shown in Fig. 2. As observed, even with a reduction of the edge length, numerical diffusion is far to be neglected, and furthermore, filling the domain with small tetrahedral elements turns the time cost too high. Mesh adaption could be a way out to the problem, but still, the time cost for reconstructing the mesh at each timestep had to be evaluated (furthermore, this option is, at present, not available in CFX).
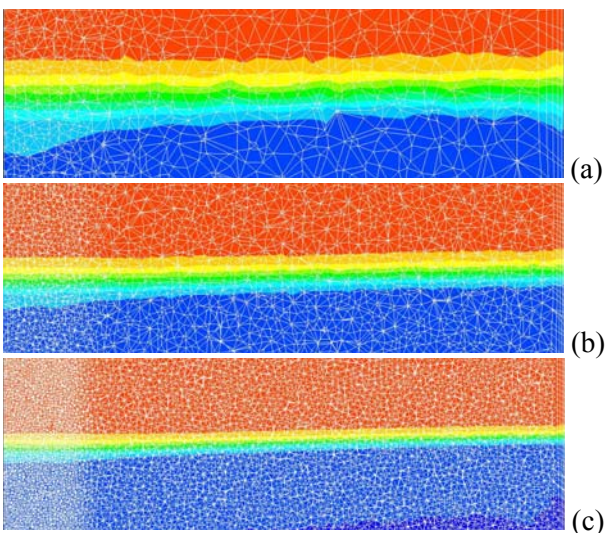
Fig. 2. Simulating a flush with ¼ cistern, using an unstructured mesh. The exit is on the bottom left. Partial view of a symmetry vertical plane with a water VOF contour (VOF=1 in blue; VOF=0 in red). Maximum edge length for the elements is: (a) 10mm; (b) 5mm and (c) 2,5mm.

The panorama gets better when a structured mesh is considered, as may be seen in Fig. 3. The interface's depth is kept around 2 elements, being sharper than that of the unstructured option and at a considerably less computational effort. Table 2 compares the number of nodes and the computer time cost for each of the meshes.

Table 2. Comparison between costs of mesh types.

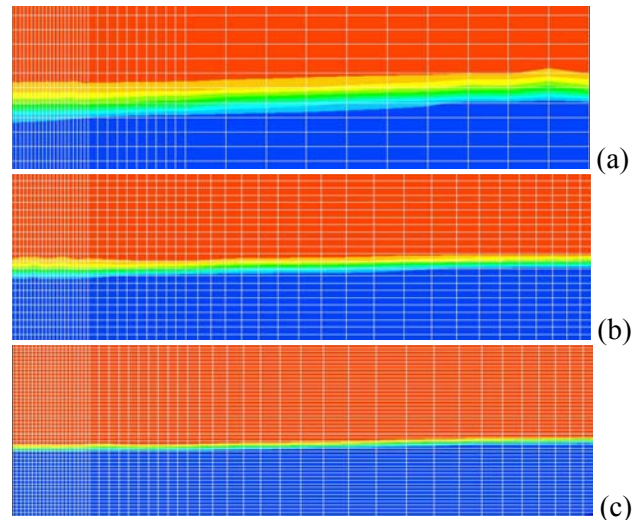| Mesh Type	Dimension [mm]	N^{er} nodes	Time cost
Unstructured	10	6903	TC_1
Unstructured	5	39055	$7,6*TC_1$
Unstructured	2,5	259694	$76,7*TC_1$
Structured	5	21525	$1,8*TC_1$
Structured	2,5	53508	$9,6*TC_1$
Structured	1,25	105924	$12,4*TC_1$

Fig. 3. Simulating a flush with ¼ cistern, using a structured mesh. The exit is on the bottom left. Partial view of a symmetry vertical plane with a water VOF contour (VOF=1 in blue; VOF=0 in red). Z dimension for the elements is: (a) 5mm; (b) 2,5mm and (c) 1,25mm, structured mesh.

Thus, it was decided to use a blend of both types of meshes. Near the valve, an unstructured mesh is employed, for a better and easy description of the geometry. In the rest of the reservoir, where a detailed description of the water free-surface is important, a structured mesh was adopted. The GGI fluid-fluid interface where both meshes join was placed in regions of low velocity gradients.

A 50 mm extension to the valve exit was introduced to prevent a local vortex to erratically lead water upstream, which would give two different behaviours depending on the type of exit chosen. An

"outlet" type of exit would create artificial walls to prevent water input which would not be physically correct and an "opening" type of exit would lead to a volume flow imprecision of nearly 45%. The domain used in the simulation for the original valve is represented in Fig. 4.

During the steady-state simulations, the gravity effect is "replaced" by an inlet velocity at the cistern top opening, matching the maximum volume flow rate measured at the experimental facility of 3.0 l/s. This value corresponds to an inlet velocity of u_{in}=0,064 m/s. With these low cost runs it is possible to measure pressure drop and locate recirculation zones. Pressure drop is evaluated between values taken at the top of the cistern and at the valve's exit. The area averaged water velocity at the valve's extension exit is also measured in order to get the mass flow rate.

To verify the 2 symmetry planes error induced, both full domain and ¼' domain were compared in a steady simulation with a very coarse grid (10mm edges in unstructured mesh and 5mm in structured mesh group). The values obtained are shown in Table 3, where u_m is the average velocity at the valve's extension exit. The averaged velocity and the pressure drop are very similar in both calculations and only 1/30 the computational effort is needed for the symmetry model. This model will be kept on the next simulations for offering an acceptable representation of the full domain with considerably less computational effort.

Table 3. Values obtained in a steady simulation for a full domain compared to the 2 symmetry planes ¼' domain.

Nodes	Δp [Pa]	u_m [m/s]	Time cost
440994	1924,73	1,378	$30*TC_2$
111567	1941,03	1,375	TC_2

In order to select the time step value and the residual target, experimental values are needed to quantify the numerical error. Unsteady simulations with refined meshes were then performed in order to measure the volume flow in a similar way than the experimental facility. Given the heights of 5 and 2 litres (h_5 and h_2, respectively) from the experimental facility, the corresponding time instants (t_5 and t_2) are obtained when a VOF=0.5 iso-surface crosses the XY planes at z=h_5 and z=h_2 (see Figure 5). These time instants are then used to obtain the volume flow as follows:

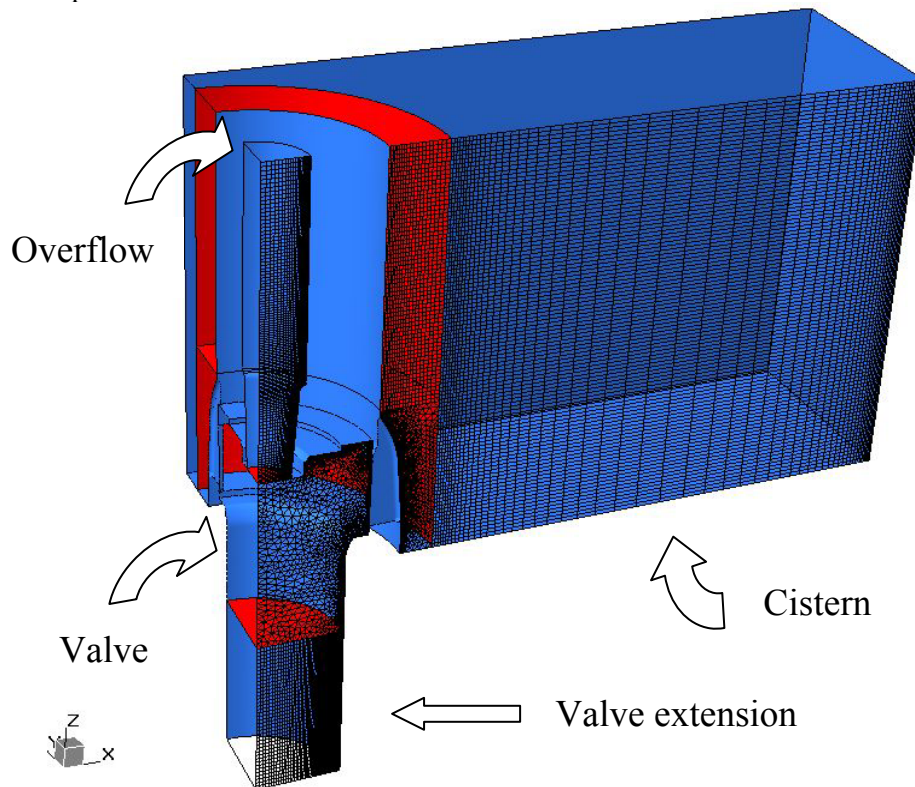$$\dot{V} = \frac{3}{t_2 - t_5} = \frac{3}{\Delta t_{num}} \quad [l/s] \quad (2)$$

Fig. 4. 3-D Model simulating ¼ of the cistern with the discharge valve. The domain is made of 5 solids connected through 4 GGI fluid-fluid interfaces (in red): the cistern (2 solids), the valve, the overflow, and the extension. An example of the mesh is shown in the ZX symmetry plane.
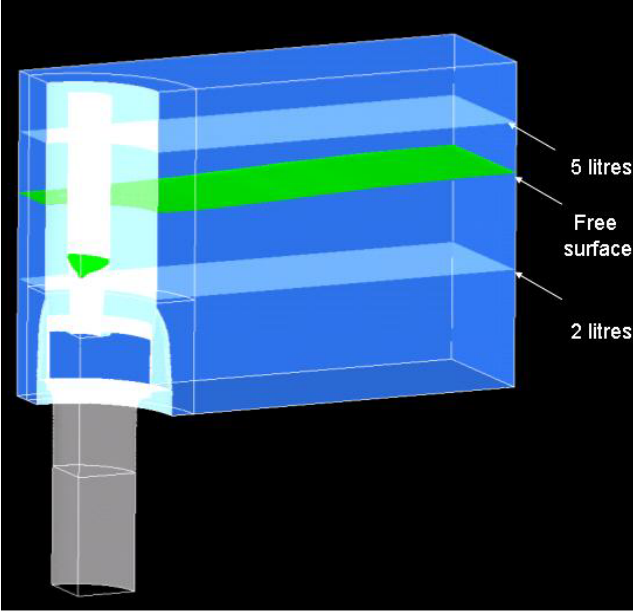
Fig. 5. Method used to measure the discharge time between 5 and 2 litres, Δt_{num}. Instants t_2 and t_5 are taken when a VOF=0.5 isosurface crosses each level respectively.

The k-ω based Shear Stress Transport (SST) is recommended for accurate predictions of the amount of flow separation under adverse pressure gradients, overcoming deficiencies in the original k-ω model. The resolution of the boundary layer must be superior to 10 points for this model to be effective.

Tests were performed on a refined mesh with 1,25 mm element height in the structured mesh and a maximum edge length of 2 mm in the unstructured mesh with several mesh controls and 15 layers boundaries in the valve's inner walls (condition needed to keep $y^+ \leq 2$ for a SST k-ω turbulence model, following the CFX user manual), giving a total number of 468685 nodes in the entire mesh.

The choice of a RMS residual target for convergence should follow some of the CFX user manual advices, as for example: MAX residual are usually a factor of 10 above RMS residuals; RMS target is specified for u, v, w and p residuals, VOF residuals will be around a factor of 10 above those; MAX residuals superior than 5×10^{-4} is very poor, giving poor global imbalances and unreliable quantitative data.

Trying to comply with these advices with a minimum computational effort, the starting simulations were made with RMS $\leq 5 \times 10^{-5}$. In fact, convergence is obtained with a maximum of 6 iteration/step. The pressure residuals are found a factor of 10 above u, v and w residuals. Numerical error from residual target will be measured later.

The choice of the time step value is based on a L/U (length/velocity) scale. The length scale is a geometric scale and the velocity scale should be the maximum between a representative flow velocity and a buoyant velocity given by:

$$U_{buoyant} = \sqrt{g.L} \qquad (3)$$

$$\Delta t = \frac{L}{U_{MAX}} ; \; U_{MAX} = MAX\left\{U, U_{buoyant}\right\} \; (4)$$

In the middle of the cistern, during the discharge between 5 and 2 litres, the mean velocity was already evaluated as u =0,064 m/s. With 1,25mm dimension in the z direction, equations (3) and (4) return 0,0113s. The steady simulation of the 468685 nodes mesh with u_{in} =0,064 m/s returns the results in Table 4.

Table 4. Results for a steady simulation of the refined 5 solids mesh.

Nodes	Δp [Pa]	u_m [m/s]	Time cost
468685	1212,31	1,4136	$8.3*TC_2$

Using the mean velocity obtained at the exit and the maximum edge length in the unstructured mesh, equations (3) and (4) return 0,0009s. The chosen values to be tested for the time step were 0,0025s; 0,005s and 0,01s (steps smaller than 0,0025s were too expensive) and results of the transient runs are shown in Table 5. The numerical error, evaluated by equation (1), and the time cost are compared.

Table 5. Results for a transient simulation of the refined mesh for different time step values.

Time step [s]	Time cost	Δt_{num} [s]	ε_{num} [%]
0.0025	$3.6*TC_3$	0.883	-4.06
0.005	$2.1*TC_3$	0.886	-4.42
0.01	TC_3	0.899	-6.00

The time step value of 0,005s already gives an acceptable relation between relative error and time cost, so, further refinement of the time step value seems unnecessary for this purpose.

The dependence of the computed discharge time with the RMS error target is shown in Table 6. One may observe that the values calculated with the procedure described previously do not change when

the RMS target is below 1×10^{-4}. Thus, the remaining computations were carried using RMS $\leq 5 \times 10^{-5}$.

Table 6. Results for a transient simulation of the refined mesh for different residual RMS target values.

RMS $\leq$	Time cost	Δt_{num} [s]	ε_{num} [%]
1×10^{-4}	TC$_4$	0,886	-4,42
5×10^{-5}	1.5*TC$_4$	0,886	-4,42
1×10^{-5}	2.25*TC$_4$	0,886	-4,42

Validation of numerical results is also made by comparing the location of the free surface during the discharge. The corresponding experimental and numerical data may be seen in Fig. 6. The numerical simulation corresponds to the 0,005s time step value, which was seen to have a relative error under 5% in Table 5. The proximity of the points in Fig. 6 confirms the reliability of the numerical model.
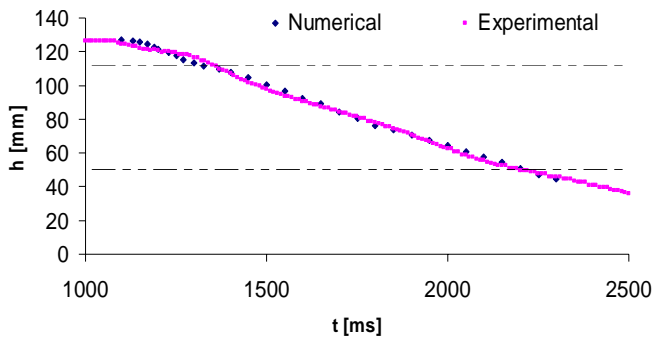

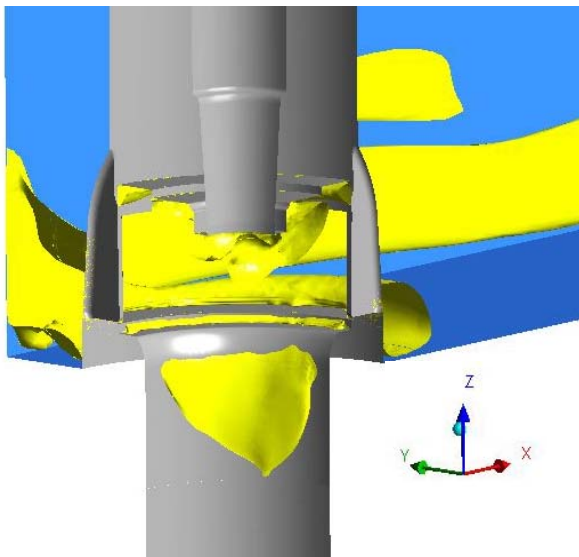Fig. 6. Dependence of the free surface position with time: experimental and numerical data.

Fig. 7. Visualisation of an isosurface for a constant value of the vertical component of the velocity (w = 0.01 m/s). Numerical results for a mesh with 468685 nodes in a stationary run

Figures 7 and 8 show numerical results, where one may appreciate the extension of the separated region near the valve exit. These results are in accordance with experimental visualisations carried out in a valve equipped with dye injectors in this region. Further experimental investigation is needed to take quantitative validation, and the use of techniques like LDA and HWA [6] could be helpful in this sense.
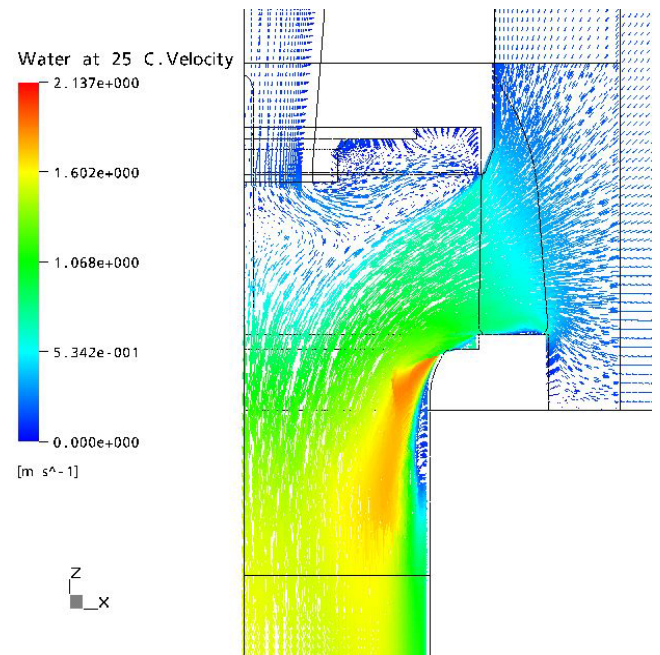

Fig. 8. Water velocity vector field. Numerical results for a mesh with 468685 nodes in a stationary run.

3.3 Valve Optimisation

Next step is to improve the valve's geometry, in order to reduce the extension of the separated region near the exit, as shown in Figures 7 and 8. This can be achieved through a reduction in the pressure drop. New shapes were built, by changing the geometric shape both in the separation regions and in the overflow exit. The goal is to decrease pressure drop and separation, to meet the manufacturer's target.

The valve shown in Figures 9 and 10 presents a good performance and is still within the allowed geometrical constrains in terms of production requirements. One can see that recirculation is well reduced in both valve's walls and overflow exit. Values obtained in a stationary simulation are compared to the original valve in Table 7. The new valve offers a better performance than the original one.

Table 7. Comparison of results between valves for a steady simulation.

Valve	Δp [Pa]	u_m [m/s]
Original valve	1212,31	1,4136
New valve	1142,03	1,4153

In order to confirm the optimisation brought with this new valve, a non-stationary simulation was conducted to get the numerical discharge time.
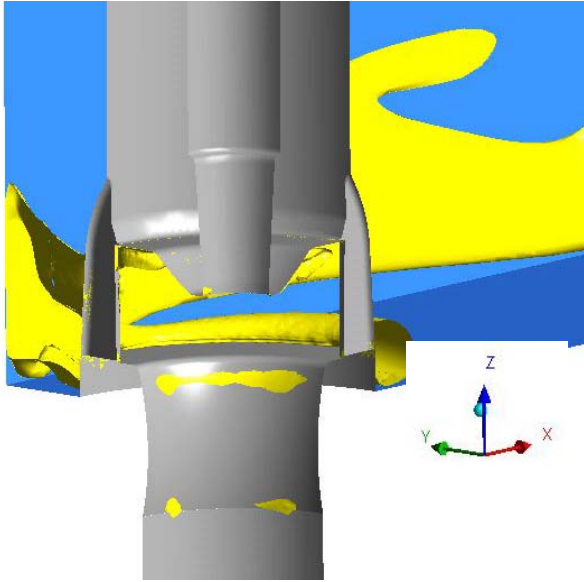

Fig. 9. Visualisation of an isosurface for a constant value of the vertical component of the velocity (w = 0.01 m/s). Numerical results for the improved valve in a stationary run
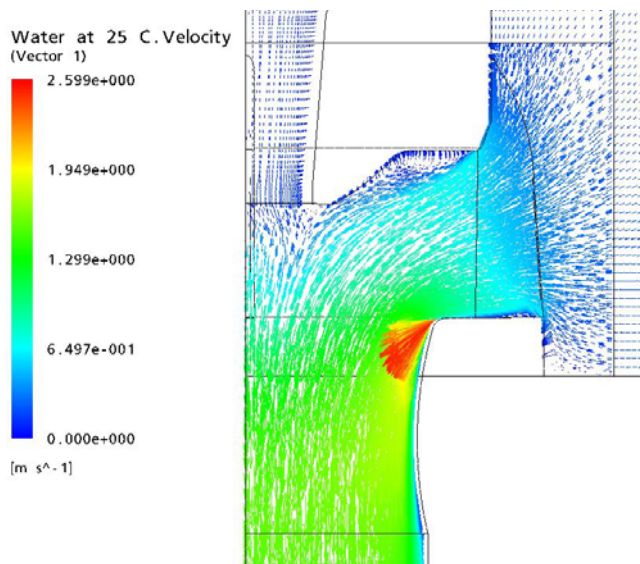

Fig. 10. Water velocity vector field. Numerical results for the improved valve in a stationary run.

The non-stationary simulation of this new valve confirmed the optimisation when a smaller value of the discharge time, $\Delta t_{num} = 0.860 s$, was obtained.

A prototype of this new valve was constructed for experimental validation of this discharge time, using the same method as described in sub-section 3.1. The results obtained are presented and compared to the original valve's results on Table 8.

Table 8. Comparison of results between valves for a transient simulation.

Valve	Δt_{exp} [s]	Δt_{num} [s]	ε_{num} [%]
Original valve	0.848	0.886	-4.42
New valve	0.821	0.860	-4.74

Looking at Table 8, one can see two things:
- The new valve confirmed to be faster than the original, both numerical and experimentally;

- The relative numerical error is, once again maintained below 5%, which confirms reproducibility and validation of the method.

Figure 11 shows the location of the free surface during the discharge using both numerical and experimental data. Both evolutions have a similar slope during the discharge, which is a good sign of correlation between results.
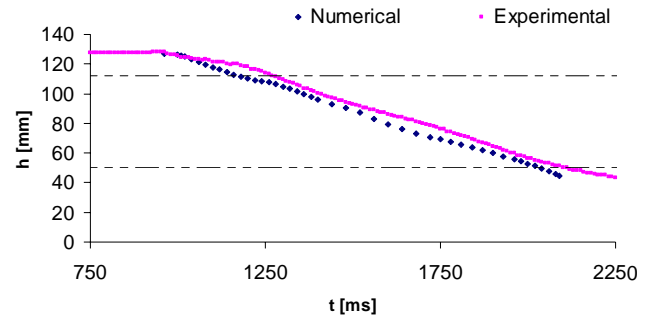
4   Conclusion

The present paper describes the methodology and preliminary tests for the numerical and experimental study of the flow in a discharge valve. The numerical simulations showed to be a quite challenging task, due to the need of a precise location of the free surface during the transient runs. The grid dependence studies showed that a blend of structured and unstructured meshes presented a good compromise for a correct description of both the valve geometry and location of the free surface. The transient simulations with a compressive scheme could predict the volume flow rate with a relative error lower than 5%.The geometry optimisation was made based on the pressure drop for stationary runs, followed by transient simulations for a correct quantification of the discharge flow rate. Experimental results of an optimized valve confirm

the relative numerical error below 5%. The methodology described in this paper could be able to predict this kind of results with the above accuracy.

References:
[1] Darwish, M., Development and testing of a robust free-surface finite volume method, *Faculty of Engineering and Architecture, American University of Beirut*, 2003.
[2] Zwart, P.J., Scheuerer, M. and Bogner, M., Free surface flow modelling of an impinging jet, *ASTAR International Workshop on Advanced Numerical Methods for Multidimensional Simulation of Two-Phase Flow*, GRS Garching, Germany, 2003.
[3] Gross, E.S., Bonaventura, L. and Rossati G., Consistency with continuity in conservative advection schemes for free surface models, *Int. J. Num. Meth. Fluids*, 38:307-327, 2002.
[4] Jongen, T. and Chouikhi, S.M., Simulation of free-surface flows induced by partially immersed moving body: Validation, *AIChE Journal*, Vol.48, No.3, 2002.
[5] Serra A., Campolo M., Soldati, A., Time-dependent finite-volume simulation of the turbulent flow in a free-surface CSTR, *Chem. Eng. Science*, Vol.56, pp.2715-2720, 2001.
[6] Weclas, M., Melling A. and Durst, F., Flow separation in the inlet valve gap of piston engines, *Prog. Energy Combust. Sci.*, Vol.24, pp.165-195, 1998.
[7] Menter, F., CFD best practice guidelines for CFD code validation for reactor-safety applications, *ECORA*, 2001.
[8] Oliveira, L.A., Cálculo Numérico de Escoamentos com Transferência de Calor e Massa, S.A.E.M. – F.C.T.U.C., 1989.
[9] Patankar, S.V., Numerical Heat transfer and Fluid Flow, Hemisphere Publishing Corporation, 1980.